Talanta 219 (2020) 121187

Contents lists available at ScienceDirect

Talanta

journal homepage: www.elsevier.com/locate/talanta

Skin ethanol gas measurement system with a biochemical gas sensor and gas concentrator toward monitoring of blood volatile compounds

Takahiro Arakawa[a,*], Takashi Aota[b], Kenta Iitani[a,c], Koji Toma[a], Yasuhiko Iwasaki[d], Kohji Mitsubayashi[a,b,**]

[a] Institute of Biomaterials and Bioengineering, Tokyo Medical and Dental University, Tokyo, Japan
[b] Graduate School of Medical and Dental Sciences, Tokyo Medical and Dental University, Tokyo, Japan
[c] Postdoctoral Research Fellow PD, Japan Society for the Promotion of Science, 5-3-1 Kojimatchi, Chiyoda-ku, Tokyo 102-0083, Japan
[d] Faculty of Chemistry, Materials and Bioengineering, Kansai University, Osaka, Japan

ARTICLE INFO

Keywords:
Gas sensor
Skin gas
Enzyme
ppb gas sensing
Biosensor
Gas concentrator

ABSTRACT

We developed a biochemical gas sensor (bio-sniffer) using the enzymatic reaction of alcohol dehydrogenase (ADH) to target ethanol in skin gas. By introducing a gas concentrator using liquid nitrogen, we constructed a highly sensitive system for skin gas measurements. The ethanol bio-sniffer was built from an optical-fiber probe employing an ADH enzyme membrane, an UV-LED light source for excitation, and a photomultiplier tube. Ethanol was measured by detecting the autofluorescence of the coenzyme NADH due to the enzymatic reaction of ADH. We established a system for measuring concentrated gases by connecting the sensor with a gas concentrator and introducing concentrated skin gas to the sensing surface. This suppressed diffusion of the concentrated gases to achieve maximum fluorescence intensity by optimizing the measurement system. The calibration curve from obtained peak values showed ethanol gas can be measured over 1–3100 ppb, which included skin gas concentrations during alcohol consumption. Finally, when applied to measurements of ethanol in skin gas following alcohol consumption, the output was found to be dependent on concentration, similarly to using standard gases. Consecutive measurements were possible using periodic sampling with 6-min intervals for 180 min of monitoring. Skin ethanol concentrations rose from 20 min after consuming the alcohol, exhibited a peak value of 25 ppb skin gas ethanol at around 60 min, and gradually declined. Thus, the system can be used for non-invasive percutaneous evaluation of human volatile organic chemicals in blood.

1. Introduction

Biological gases such as exhaled air and skin gas contain volatile organic compounds (VOCs) derived from components of the blood [1,2]. Since these are the products of metabolism or disease, in recent years, the measurement of human VOCs in skin gas and exhaled air has been considered a useful method for simple and non-invasive metabolism sensing and disease screening [3–5]. Skin gas is easier to collect than exhaled air and, since there is less restriction during measurement, it is possible to evaluate the biological condition of a subject while placing little burden on them [6–8]. However, the VOCs contained in skin gas have extremely low concentrations and smaller sample amounts are obtained compared to exhaled air [9]. For example, while the concentration of acetone in the exhaled air of healthy individuals at rest is 200–900 ppb, the concentration in skin gas has been reported to be around 77–97 ppb [10,11]. In addition, the concentration of ethanol in the exhaled air of healthy individuals at rest is 37–207 ppb, whereas the concentration in skin gas is extremely low, at 3.6–79.2 ppb/min, even when measuring the upper arm and the whole hand [12,13]. As such, since the ethanol and acetone released from the skin have very low concentrations of a few tens of parts per billion, there is demand for highly sensitive gas measurement techniques [13–16].

Biological gases of human VOCs, including those other than skin gas, are mixtures of many components, the concentrations of which fluctuate over time, and their measurement requires sensitive and responsive devices with excellent selectivity for gases and that can

* Corresponding author. Takahiro Arakawa Department of Biomedical Deviced and Instrumentation, Institute of Biomaterials and Bioengineering, Tokyo Medical and Dental University, 2-3-10 Kanda-Surugadai, Chiyoda-ku, Tokyo, 101-0062, Japan.
** Corresponding author. Department of Biomedical Deviced and Instrumentation, Institute of Biomaterials and Bioengineering, Tokyo Medical and Dental University, 2 Kanda-Surugadai, Chiyoda-ku, Tokyo, 101-0062, Japan.
E-mail addresses: arakawa.bdi@tmd.ac.jp (T. Arakawa), m.bdi@tmd.ac.jp (K. Mitsubayashi).

https://doi.org/10.1016/j.talanta.2020.121187
Received 10 February 2020; Received in revised form 16 May 2020; Accepted 16 May 2020
Available online 30 May 2020
0039-9140/

measure continuously. At present, research into skin gas has used gas chromatography with mass spectroscopy and semiconductor sensors; however, these have issues such as being complicated to operate, being unsuited for continuous measurements, and having poor gas selectivity. It is therefore difficult to continuously measure skin gas components simply with high sensitivity [17–20].

We have reported on research regarding biochemical gas sensors (bio-sniffers) and is making progress in the fields of highly sensitive and selective gas component measurement in exhaled air, the evaluation of metabolism through these measurements, and the visualization of changes over space and time [21–25]. In the measurement of VOCs in skin gas, it has been reported that liquid nitrogen was used to concentrate acetone in skin gas for highly sensitive measurements [10]. In other words, concentrating skin-derived biological gas samples and loading this in the bio-sniffer may enable highly sensitive measurement of skin gas VOC components. In our previous study, we developed a skin gas monitoring system with detection limit of 25 ppb ethanol gas [23]. However, measurement of low concentration of ethanol gas below 10 ppb has not been realized.

Consequently, in the present study, in order to enable percutaneous, non-invasive evaluation of alcohol metabolism targeting ethanol contained in skin gas, we established a system for skin ethanol measurements by combining an ethanol bio-sniffer with a gas concentrator. After evaluating the characteristics of the sensor using standard ethanol gas, we applied the system to the measurement of ethanol in skin gas following the consumption of alcohol to investigate the possibility of using the system for metabolic sensing.

2. Experimental

2.1. Construction of the system for skin ethanol measurement

We used alcohol dehydrogenase (ADH), which catalyzes the oxidation of ethanol, to measure ethanol gas. In the oxidation of ethanol (Eq. (1)), ADH reduces the coenzyme, oxidized NAD (NAD^+), to produce reduced NAD (NADH), which autofluoresces (ex. 340 nm, fl. 491 nm). Thus, we decided to measure the ethanol gas by detecting the change in NADH-derived fluorescence intensity due to the enzymatic reaction.

$$\text{ethanol} + NAD^+ \xrightarrow{ADH} \text{acetaldehyde} + NADH + H^+ \quad (1)$$

As shown in Fig. 1(a), the skin ethanol measurement system is constructed from an optical-fiber probe equipped with a flow cell, an exciting light source comprising an ultraviolet light-emitting diode (UV-LED, λ = 340 nm), a photomultiplier tube (PMT), a band-pass filter (BPF), a standard gas generator (permeator, GASTEC Co.), and a gas concentrator (NIT-P, Pico-Device. Co.). The excitation system utilized a UV-LED (UF4VL-1H33, Dowa Electronics Materials Co.) with a UV-LED power supply circuit (GS200, Yokogawa Electric Cor-poration, Japan). The tip of the flow cell was equipped with a membrane with immobilized S-ADH and fed using a buffer solution containing NAD^+ as the liquid phase. The membrane with immobilized ADH enzyme was prepared using a hydrophilic and porous H-PTFE membrane (pore size 0.2 μm, thickness 80 μm) as the supporting membrane (Omnipore, Merck KGaA). Entrapment immobilization of ADH used poly[MPC-co-EHMA] (PMEH), a copolymer of 2-methacryloyloxyethyl phosphorylcholine (MPC) and 2-ethylhexyl methacrylate (EHMA). During this process, a mixture of 10 μl/cm^2 enzyme solution containing ADH (128 units/mg solid) and 10 μl/cm^2 of 15% PMEH was applied (60 units/cm^2) to the H-PTFE membrane.

Gas concentrators can cool sample gases using liquid nitrogen to concentrate their VOC components to a volume of 0.1 ml. The device has a cryostat that can maintain a low temperature of −50 °C in the part of the device where the sample gas and liquid nitrogen paths run parallel, thereby enabling concentration of the sample gas. When not concentrated, the carrier gas flows through the path including the cryostat and reaches the sensing surface However, once the concentration has begun, the flow path is switched such that the sample gas and liquid nitrogen are taken in and the inside of the cryostat is cooled by the liquid nitrogen, concentrating the components within the sample gas and liquefying them (Fig. 1(b)). Following concentration, the cryostat is heated to 100 °C, vaporizing the liquefied components within the cryostat. The cryostat is heated to 100 °C to vaporize all the concentrated volatile components. Simultaneously, the carrier gas path is connected to the cryostat, thereby introducing the concentrated gas to the sensing surface.

When the concentrated ethanol gas from the gas concentrator is loaded onto the sensing surface, NADH is produced from NAD^+ in the buffer solution, owing to the enzymatic reaction of S-ADH on the enzyme membrane. The UV-LED light is passed through a BPF (λ = 340 ± 10 nm) and the tip of the optical-fiber probe to illuminate the NADH with 340 nm excitation light, generating fluorescence from the NADH with a central wavelength of 491 nm. This fluorescence is focused through the end of the optical-fiber probe through another BPF (λ = 490 ± 10 nm) and detected by the PMT to enable quantification of the ethanol. These components were connected to separated ends of a bifurcated optical fiber assembly (core size 400 μm, BIF400-UV-VIS, Ocean Optics Inc. USA).

In this experiment, the characteristics of the system were checked by concentrating 1 ppm standard ethanol gas with multiple scaling factors and loading this on the sensing surface. Subsequently, we performed some optimizations (of the gas phase cell and flow cell volumes, the length of the carrier gas tubing, the inner diameter of the tubing, and the carrier gas flow rate) and also investigated the suppression of diffusion of the concentrated gas. Next, we also optimized the buffer solution flow rate and the current applied to the excitation light source in an effort to improve the intensity of the output fluorescence.

First, the 1 ppm standard ethanol gas was concentrated 2-, 50-, 500-, and 1000-fold, and loaded on the sensing surface with a carrier gas (50 ml/min) to confirm that the output peak values corresponded to the concentration ratio. Next, to prevent diffusion of the concentrated gas at the sensing surface and improve the fluorescence intensity generated by the ethanol gas, we miniaturized the gas phase cell that acts as the part that senses ethanol gas and the flow cell attached to the end of the optical-fiber probe (Fig. S1). The diameter of the optical fiber of the flow cell was reduced (6.0–1.6 mm), lowering the internal diameter of the cell from 11.5 mm to 6.0 mm (area: 20%). In addition, the volume of the sensing part of the gas phase cell was reduced to around 17% (1500 to 250 mm^3), reducing the effect of diffusion. Next, the 1 ppm standard ethanol gas was concentrated (250- to 1000-fold) and loaded on the sensing surface with a carrier gas to evaluate the effect of diffusion on the concentrated gas.

In addition, lengths of 150 and 1000 mm were used for the tubing of the carrier gas path from the gas concentrator to the sensing surface. The influences of changes to the internal diameter of the carrier gas path tubing and the dry air flow rate on the output were investigated. The buffer solution flow rate within the flow cell was also reduced in an effort to improve the intensity of fluorescence detected by the PMT per unit time. Furthermore, the current applied to the UV-LED was optimized for this system to improve NADH fluorescence intensity.

2.2. Evaluation of the characteristics of the system for skin ethanol measurement

We evaluated the quantitative characteristics for standard ethanol gas, in addition to the responsiveness and selectivity of the system. In the evaluation of the calibration curve and responsiveness, the standard gas generator was used to prepare various concentrations of ethanol gas (1–3100 ppb), which was concentrated 1500-fold by the concentrator and loaded on the sensing surface, upon which the change in fluorescence intensity was measured. To evaluate the selectivity, we prepared

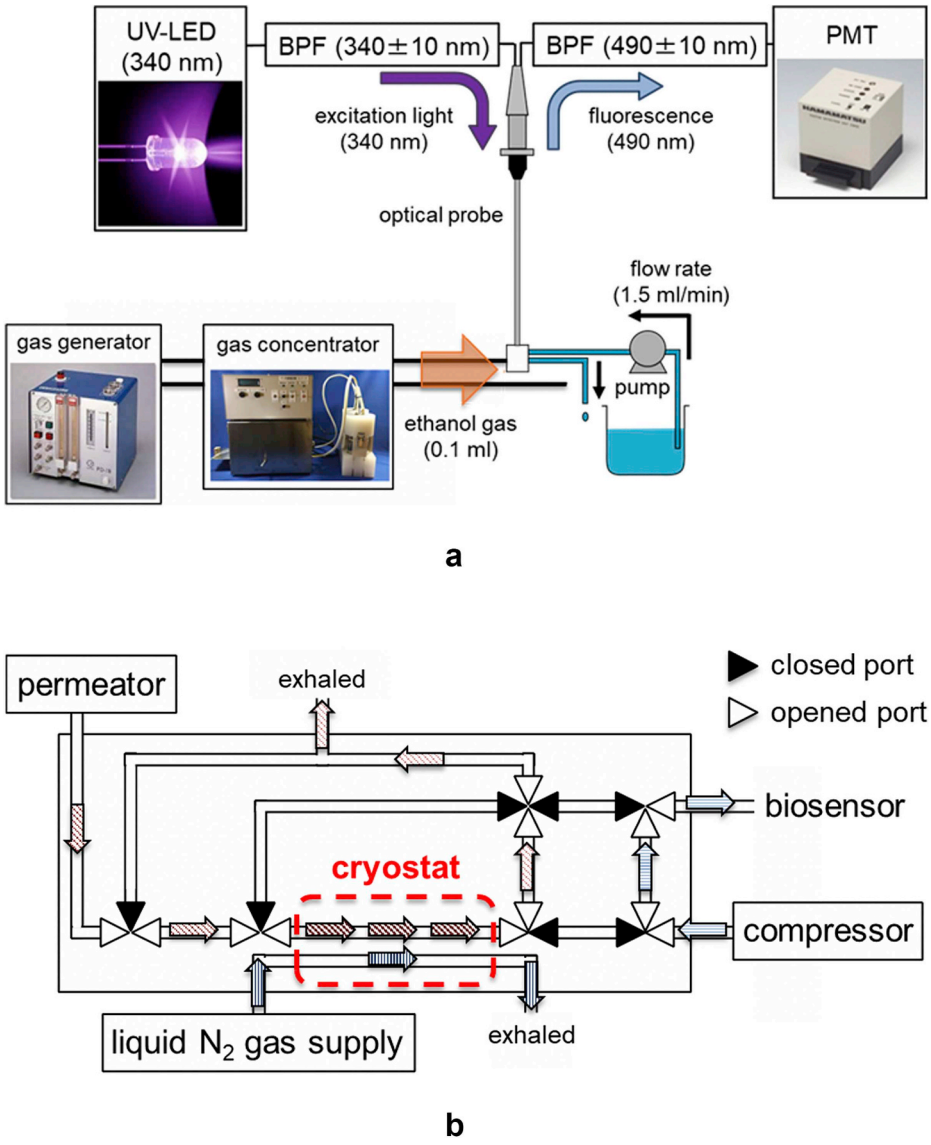

Fig. 1. Schematic illustration of skin ethanol gas measurement system using a bio-sniffer and gas concentrator (a) system for measurement of skin gas using a gas concentrator. (b) internal structure of the gas concentrator and the path during concentration.

typical exhaled air components with concentrations appropriate for exhaled air and loaded them on the sensing surface to compare the output.

2.3. Periodic monitoring of ethanol in skin gas

The constructed system was tested for biological applications by performing periodic measurements of ethanol in skin gas following the consumption of alcohol (Ethics Review Committee of the Institute of Biomaterials and Bioengineering, Tokyo Medical and Dental University; approval number: 2012–6 (M2018-160)).

For the alcohol consumption experiment, the objective was explained in advance and consent obtained from healthy adult subjects, who completed a questionnaire and performed an alcohol patch test in advance, and were classified by whether they were ALDH2[+] (active) or [−] (inactive), after which the experiment was performed on those subjects who were able to undergo it. The alcohol used in the experiment was consumed orally as an alcoholic beverage (consumed alcohol: 0.4 g per 1 kg of body mass) by subjects who had fasted for three or more hours and had not taken any medicines or drank alcohol within the last 72 h.

To investigate the dynamics of the release of ethanol contained in skin gas, a skin gas collection cell ("skin cell") was used for skin measurements. The skin cell used a Teflon cell with a skin gas collection area of 10 cm^2 and double-sided tape was adhered to the cell's skin-contacting side to fix it tightly against the skin surface (Fig. 2). To introduce the skin cell gas to the device, we constructed the system such that dry compressed air was used as a carrier gas by pumping the air (150 ml/min) to the concentrator when concentrating the gas and expelling the air through a one-way valve installed near the concentrator inlet when not concentrating. The wrist was used as the skin gas measuring location, as this was found to be appropriate for continuous measurement in prior research [23]. The skin gas was concentrated and loaded on the sensor every 6 min and we regularly measured the changes in skin gas ethanol concentration over time (from 20 min prior to consuming alcohol to 3 h after).

In addition, exhaled air gas measurements were performed simultaneously and the dynamics of ethanol release in exhaled air and skin gas were compared. For the exhaled air measurements, exhaled air was collected using sample bags as appropriate and the ethanol

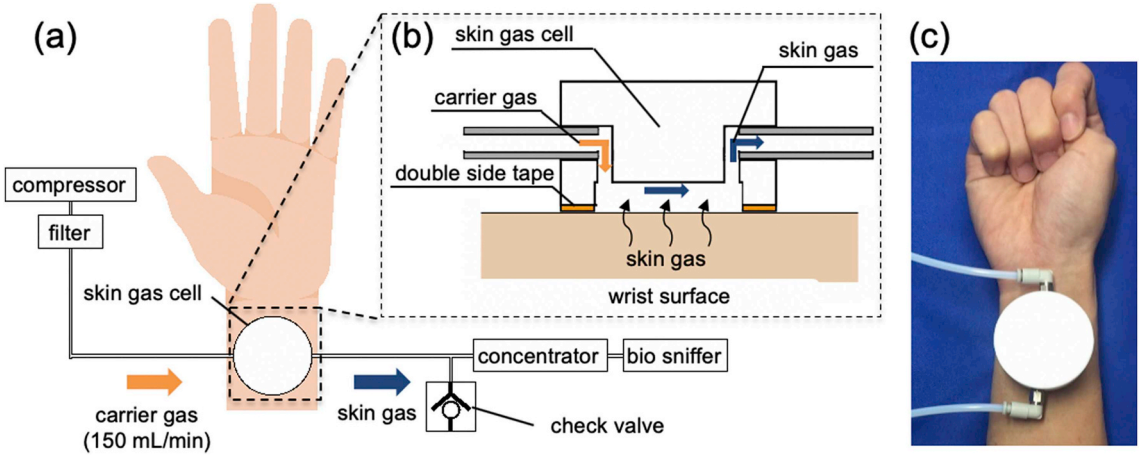

Fig. 2. (a) Schematic overview of the skin gas measurement system using the skin cell. (b) Schematic of cross-sectional view of skin gas being collected from the wrist. (c) the skin-cell wearing image.

concentration was measured using a gas detector tube (112 L, Gastec Co.).

3. Results and discussion

3.1. Optimization and evaluation of the system for skin ethanol measurement

Fig. S2 shows the responsiveness when 1 ppm standard ethanol gas was concentrated 250- to 1000-fold and loaded on the sensing surface of the system. As shown in Fig. S2, the increase in the fluorescence intensity peak value is determined by the concentration ratio set by the gas concentrator. However, the fluorescence intensity peak value was low, which we thought to be the influence of diffusion of the concentrated gas and therefore we investigated the suppression of diffusion of the gas.

Consequently, we investigated the suppression of diffusion of the gas by miniaturizing the gas phase cell and flow cell. Fig. S3 shows a comparison of the output values for concentrated ethanol gas (250–1000 ppb) using two gas phase cell volumes (250 and 1500 mm^3) for the system. It was found that, after reducing the volumes of the gas phase cell and flow cell, the output values were higher than before the volume reduction, with the peak value of the output increasing 1.6-fold for the concentration corresponding to 500 ppb. This result suggested that the miniaturization of the gas phase cell and the flow cell suppressed diffusion of the concentrated gases at the sensing surface, elevating the peak output. Consequently, we decided to use a volume of 250 mm^3 for the gas phase cell in subsequent experiments.

Next, we investigated how the output is influenced by the length of the carrier gas path tubing from the gas concentrator to the sensing surface. In this experiment, we compared two gas tubing lengths (150 and 1000 mm) for the system while loading with concentrated ethanol gas (250–1000 ppb). Fig. S4(a) shows the results for the gas tubing length of 150 mm and, as can be deduced from the figure, a highly reproducible output was observed that depended upon the concentration. Fig. S4(b) compares the results for the two gas tubing lengths (150 and 1000 mm). As shown in the figure, for concentrated 500 ppb ethanol gas, a 1.4-fold higher output was observed for the gas tubing length of 150 mm compared to 1000 mm. The above confirmed that the fluorescence intensity could be increased by suppressing diffusion of the gas between the sensing surface and the concentrator by selecting shorter gas tubing lengths. Therefore, we decided to use a gas tubing length of 150 mm for subsequent experiments.

We also investigated the internal diameter of the gas tubing and the carrier gas flow rate. We set up two internal diameters (ϕ0.5 and ϕ1.0 mm) and various carrier gas flow rates (10, 20, 50 ml/min) for the system while loading with concentrated ethanol gas (250–1500 ppm). The results of the experiment confirmed that an internal tubing diameter of ϕ0.5 mm and a carrier gas flow rate of 20 ml/min led to the maximum fluorescence intensity. This is because reducing the internal diameter of the tubing increased the gas flow rate, enabling a low carrier gas flow to carry the concentrated gas to the sensing surface. Upon comparing with the output for 1500 ppm ethanol gas under the previous conditions (an internal tubing diameter of ϕ1.0 mm and a flow rate of 50 ml/min), it was found that the output had increased 1.2-fold. For subsequent experiments, we decided to use an internal tubing diameter of ϕ0.5 mm and a carrier gas flow rate of 20 ml/min.

When using a flow rate of 10 μl/min to feed the buffer solution into the flow cell, reducing the flow rate was observed to increase the output and delay recovery times to the initial value. The delay was due to NADH produced by reactions in the flow cell staying in the flow cell longer at reduced flow rates, which also led to a greater intensity of fluorescence being observed. Next, we evaluated the output and responsiveness upon changing the buffer solution flow rate. Fig. 3 shows the relationship between the output and responsiveness for concentrated ethanol gas (1 ppm × 250) using various buffer solution flow rates (0.5 μl/min to 1.0 ml/min). As can be deduced from the figure, the fluorescence intensity is high at a buffer flow rate of 5 μl/min and takes a short time to recover to its initial value. Consequently, we decided to use a buffer flow rate of 5 μl/min for subsequent experiments.

Finally, we investigated the effect of the current applied to the UV-LED used as the excitation light source. We investigated the influence of

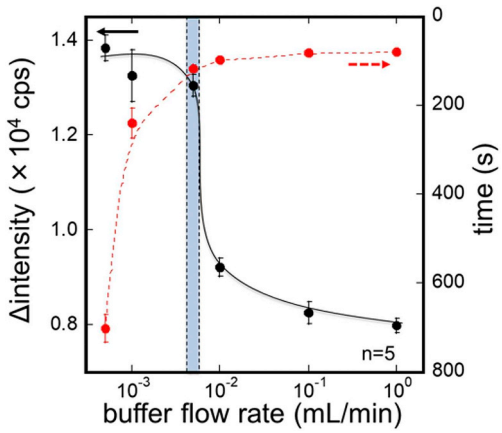

Fig. 3. The relationship between the output and responsiveness for concentrated ethanol gas (1 ppm × 250) using various buffer solution flow rates (0.5 μl/min to 1.0 ml/min).

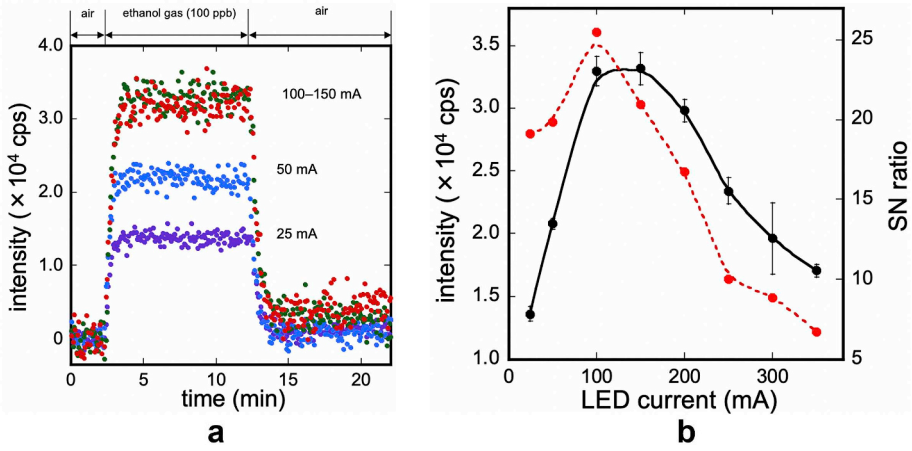

Fig. 4. Optimization of the condition of UV-LED (a) The responsiveness of the bio-sniffer for 100 ppb ethanol gas when applying currents of 25–150 mA to the UV-LED. (b) Changes to the output and SN ratio versus the applied current between 25 and 350 mA.

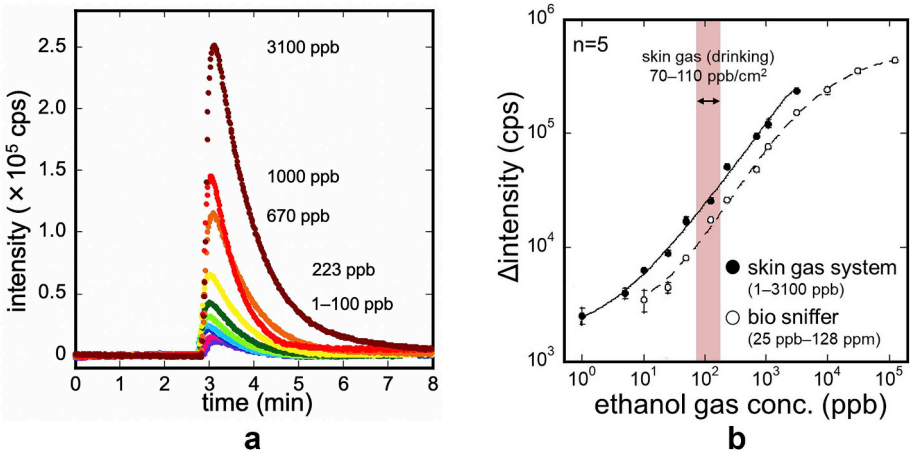

Fig. 5. Characteristics of the developed skin gas system with ADH bio-sniffer and the gas concentrator (a) The output response of the ADH bio-sniffer to various concentrations of ethanol gas. (b) Comparison of the calibration curve of the skin gas system and conventional ADH bio-sniffer for ethanol gas.

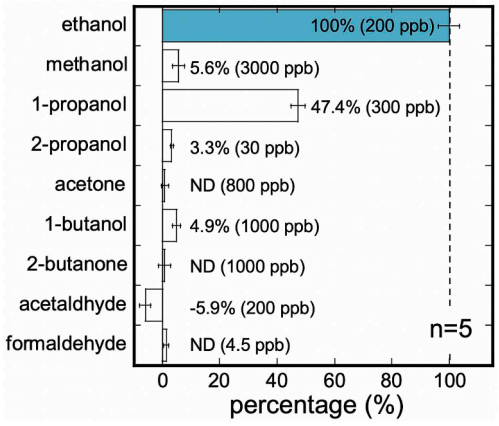

Fig. 6. Comparison of the output of the bio-sniffer for exhaled air components.

changing the current applied to the UV-LED on the output and signal-to-noise (SN) ratio. Fig. 4(a) shows the changes in responsiveness for 100 ppb standard ethanol gas when applying various currents (25–150 mA). In addition, as shown in Fig. 4(b), the fluorescence intensity reached a peak at an applied current of 100–150 mA and the SN ratio was maximized at 100 mA. The increase in the SN ratio up to an applied current of 100 mA was due to increased fluorescence intensity from the increase in light from the excitation light source. In addition, the reduction in the SN ratio for applied currents of 100 mA and above was likely due to increased noise due to light signals associated with heating of the UV-LED caused by the increase in the applied current. Based on the values for the SN ratio, in this system, we decided to use an applied current of 100 mA for the UV-LED.

3.2. Evaluation of the ethanol gas measurement system

The responsiveness and calibration curve of the system for measuring concentrated gas for its target of ethanol gas are shown in Fig. 5(a). A rapid rise in the output associated with loading of the gas and a concentration-dependent peak value were observed in addition to recovery to the initial value after the provision of gas. Based on the above results, we investigated the calibration curve for ethanol gas using the peak value as the output value. In this investigation, it was possible to quantify ethanol gas for the concentration range of 1–3100 ppb, which includes the ethanol concentration of air exhaled at rest (37–207 ppb) [12] and the maximum skin ethanol gas concentration during drinking (73.9–112.1 ppb/cm^2) [26] (Fig. 5(b)). The equation for quantifying the ethanol gas concentration for the system (Eq. (2)) (R = 0.995) is shown below.

$$\Delta\text{intensity (cps)} = 1.63\times10^3 + (2.35\times10^5 - 1.63\times103) /1 + 2.27\times103/[\text{ethanol conc. (ppb)}])^{-12.18)0.06} \quad (2)$$

In addition, compared to conventional bio-sniffers (which have determination limits of 25 ppb–128 ppm) [23,27], the lower limit of the

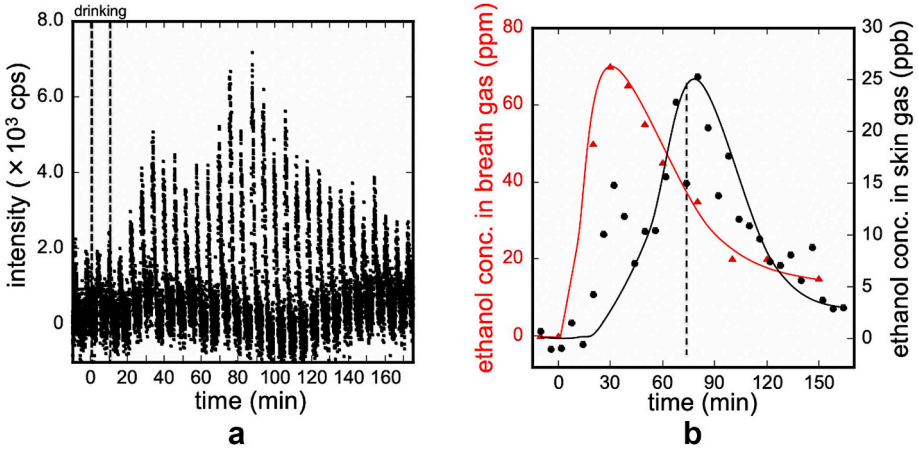

Fig. 7. The signal due to ethanol in skin gas from the wrist detected using the skin gas measurement system. (b) The ethanol concentrations in the skin gas as calculated from the peak values and the ethanol concentrations in the exhaled air calculated using a gas detector tube.

1.0 ppb detection sensitivity of the system for measuring concentrated gas that we developed was enhanced by around 25-fold.The signal-to-noise ratio was greatly improved, making it possible to measure low fluorescence signals even at low concentrations.

The selectivity of the ethanol bio-sniffer with respect to VOC gases is shown in Fig. 6. The figure shows a comparison of the outputs for non-ethanol gases (the concentrations of which are that of exhaled air or the limit of the concentration that can be produced by the permeator), where the output for 200 ppb ethanol gas is set to 100%. As shown in the figure, ethanol exhibits a high output and, although 1-propanol exhibited 47.4% of this at 300 ppb, other components exhibited almost no output. Therefore, gas selectivity was achieved thanks to the substrate specificity of the enzyme. Moreover, the concentration of 1-propanol in air exhaled by humans has been reported to be around 8.1 ppb, so it likely has little effect on biological ethanol gas measurements [28].

3.3. Skin gas cell for ethanol gas measurement

Using the concentrated gas measurement system, we applied the measurement of ethanol in skin gas to alcohol consumption. Upon performing periodic measurements of ethanol in skin gas by attaching the skin cell to the wrist, periodic output peak values dependent upon the concentration of ethanol in the skin gas were observed, as shown in Fig. 7(a). Fig. 7(b) shows the ethanol concentrations calculated and plotted using the obtained peak values. As can be deduced from the figure, it was observed that ethanol concentrations rose from 20 min after consuming the alcohol, exhibited a peak value at around 60 min after consuming the alcohol, and gradually declined thereafter. Moreover, the skin ethanol gas concentration (approximately 25 ppb) after alcohol consumption was almost the same as the results of prior research [13,29]. In addition, during the measurement of the skin gas, exhaled air was collected every 10 min and, upon investigating the concentration of ethanol in the exhaled air after alcohol consumption using a gas detector tube, it was found that, compared to the exhaled air-derived ethanol, the changes in ethanol derived from skin gas from the wrist exhibited a delay of several tens of minutes.

The above findings demonstrated that it was possible to use this concentrated gas measurement system for highly sensitive measurements of ethanol in skin gas from the wrist. Furthermore, this suggests that it is possible to perform highly sensitive measurements of small amounts of metabolic products in the skin gases, and thereby perform metabolic sensing.

4. Conclusion

We constructed a system for measuring concentrated gases by combining an ethanol bio-sniffer with a gas concentrator. To suppress the diffusion of the concentrated gas in the system, we optimized the gas tubing length (150 mm), the internal diameter of the tubing (0.5 mm), and the carrier gas flow rate (20 ml/min). In addition, to improve the sensitivity of fluorescence detection, we optimized the flow rate of the buffer solution fed into the flow cell (5 μl/min). Upon evaluating the calibration curve of the optimized system, we found that it was possible to quantify ethanol gas in the range of 1–3100 ppb, which includes the skin gas concentrations during alcohol consumption (70–110 ppb). Next, upon applying the constructed system to the measurement of skin ethanol gas from the wrist, it was possible to perform periodic measurements of ethanol concentrations in the skin gas. This result was equivalent to that of prior research and suggests that it is possible to measure blood ethanol non-invasively through the skin and evaluate alcohol metabolism. In the future, the system may enable non-invasive metabolic sensing and the early diagnosis of diseases by applying this system to the percutaneous measurement of various blood gases.

Credit author statement

Takahiro Arakawa: Conceptualization, Methodology, Writing-Original draft preparation, Investigation, Funding acquisition. Takashi Aota: Validation, Formal analysis, Investigation, Visualization. Kenta Iitani: Software, Validation, Formal analysis. Koji Toma: Resources, Data curation. Yasuhiko Iwasaki: Resources. Kohji Mitsubayashi: Project administration, Supervision, Writing - review & editing.

Declaration of competing interest

The authors declare that they have no known competing financial interests or personal relationships that could have appeared to influence the work reported in this paper.

Acknowledgments

This work was partly supported by Japan Society for the Promotion of Science (JSPS) KAKENHI Grant Number 16KK0143 and 19H02150 by the Ministry of Education, Culture, Sports, Science and Technology (MEXT).

Appendix A. Supplementary data

Supplementary data to this article can be found online at https://doi.org/10.1016/j.talanta.2020.121187.

References

[1] W.M. Ahmed, O. Lawal, T.M. Nijsen, R. Goodacre, S.J. Fowler, Exhaled volatile organic compounds of infection: a systematic review, ACS Infect. Dis. 3 (2017) 695–710, https://doi.org/10.1021/acsinfecdis.7b00088.

[2] M. Mayer, A.J. Baeumner, A megatrend challenging analytical chemistry: biosensor and chemosensor concepts ready for the internet of things, Chem. Rev. 119 (2019) 7996–8027, https://doi.org/10.1021/acs.chemrev.8b00719.

[3] Y.Y. Broza, L. Zuri, H. Haick, Combined volatolomics for monitoring of human body chemistry, Sci. Rep. 4 (2014) 2–7, https://doi.org/10.1038/srep04611.

[4] C.K. Fan, J. Losonczy, Matchings and canonical forms for symmetric tensors, Adv. Math. 117 (1996) 228–238, https://doi.org/10.1006/aima.1996.0010.

[5] S.I. Ohira, K. Toda, Micro gas analyzers for environmental and medical applications, Anal. Chim. Acta 619 (2008) 143–156, https://doi.org/10.1016/j.aca.2008.05.010.

[6] T. Tsuda, T. Ohkuwa, H. Itoh, Findings of skin gases and their possibilities in healthcare monitoring, Gas Biol Res Clin Pract (2011) 125–132, https://doi.org/10.1159/000321953.

[7] F.M. Schmidt, O. Vaittinen, M. Metsälä, M. Lehto, C. Forsblom, P.H. Groop, et al., Ammonia in breath and emitted from skin, J. Breath Res. 7 (2013), https://doi.org/10.1088/1752-7155/7/1/017109.

[8] C. Di Natale, R. Paolesse, E. Martinelli, R. Capuano, Solid-state gas sensors for breath analysis: a review, Anal. Chim. Acta 824 (2014) 1–7, https://doi.org/10.1016/j.aca.2014.03.014.

[9] N.P. Shetti, S.D. Bukkitgar, K.R. Reddy, C.V. Reddy, T.M. Aminabhavi, ZnO-based nanostructured electrodes for electrochemical sensors and biosensors in biomedical applications, Biosens. Bioelectron. 141 (2019) 111417, , https://doi.org/10.1016/j.bios.2019.111417.

[10] N. Yamane, T. Tsuda, K. Nose, A. Yamamoto, H. Ishiguro, T. Kondo, Relationship between skin acetone and blood β-hydroxybutyrate concentrations in diabetes, Clin. Chim. Acta 365 (2006) 325–329, https://doi.org/10.1016/j.cca.2005.09.016.

[11] P.R. Galassetti, B. Novak, D. Nemet, C. Rose-Gottron, D.M. Cooper, S. Meinardi, et al., Breath ethanol and acetone as indicators of serum glucose levels: an initial report, Diabetes Technol. Therapeut. 7 (2005) 115–123, https://doi.org/10.1089/dia.2005.7.115.

[12] J.D. Fenske, S.E. Paulson, Human breath emissions of VOCs, J. Air Waste Manag. Assoc. 49 (1999) 594–598, https://doi.org/10.1080/10473289.1999.10463831.

[13] P. Mochalski, J. King, K. Unterkofler, H. Hinterhuber, A. Amann, Emission rates of selected volatile organic compounds from skin of healthy volunteers, J Chromatogr B Anal Technol Biomed Life Sci 959 (2014) 62–70, https://doi.org/10.1016/j.jchromb.2014.04.006.

[14] H.G. Giles, S. Meggiorini, G.E. Renaud, J.J. Thiessen, E.I. Vidins, K.V. Compton, et al., Ethanol vapor above skin: determination by a gas sensor instrument and relationship with plasma concentration, Alcohol Clin. Exp. Res. 11 (1987) 249–253, https://doi.org/10.1111/j.1530-0277.1987.tb01300.x.

[15] J.C. Anderson, The kinetics of transdermal ethanol exchange, J. Appl. Physiol. 100 (2006) 649–655, https://doi.org/10.1152/japplphysiol.00927.2005.

[16] H. Wiesenhofer, M. Allers, S. Zimmermann, A.T. Güntner, N.J. Pineau, W. Lederer, et al., Monitoring of selected skin- and breath-borne volatile organic compounds emitted from the human body using gas chromatography ion mobility spectrometry (GC-IMS), J. Chromatogr. B 1076 (2018) 29–34, https://doi.org/10.1016/j.jchromb.2018.01.013.

[17] N. Krone, B.A. Hughes, G.G. Lavery, P.M. Stewart, W. Arlt, C.H.L. Shackleton, Gas chromatography/mass spectrometry (GC/MS) remains a pre-eminent discovery tool in clinical steroid investigations even in the era of fast liquid chromatography tandem mass spectrometry (LC/MS/MS), J. Steroid Biochem. Mol. Biol. 121 (2010) 496–504, https://doi.org/10.1016/j.jsbmb.2010.04.010.

[18] C. Wang, C. Ke, X. Wang, C. Chi, L. Guo, S. Luo, et al., Noninvasive detection of colorectal cancer by analysis of exhaled breath, Anal. Bioanal. Chem. 406 (2014) 4757–4763, https://doi.org/10.1007/s00216-014-7865-x.

[19] R. Zhang, W. Huang, G. Li, Y. Hu, Noninvasive strategy based on real-time in vivo cataluminescence monitoring for clinical breath analysis, Anal. Chem. 89 (2017) 3353–3361, https://doi.org/10.1021/acs.analchem.6b03898.

[20] B. Buszewski, T. Ligor, T. Jezierski, A. Wenda-Piesik, M. Walczak, J. Rudnicka, Identification of volatile lung cancer markers by gas chromatography-mass spectrometry: comparison with discrimination by canines, Anal. Bioanal. Chem. 404 (2012) 141–146, https://doi.org/10.1007/s00216-012-6102-8.

[21] T. Arakawa, K. Kita, X. Wang, K. Miyajima, K. Toma, K. Mitsubayashi, Chemiluminescent imaging of transpired ethanol from the palm for evaluation of alcohol metabolism, Biosens. Bioelectron. 67 (2015) 570–575, https://doi.org/10.1016/j.bios.2014.09.045.

[22] K. Iitani, T. Sato, M. Naisierding, Y. Hayakawa, K. Toma, T. Arakawa, et al., Fluorometric sniff-cam (Gas-Imaging system) utilizing alcohol dehydrogenase for imaging concentration distribution of acetaldehyde in breath and transdermal vapor after drinking, Anal. Chem. 90 (2018) 2678–2685, https://doi.org/10.1021/acs.analchem.7b04474.

[23] T. Arakawa, T. Suzuki, M. Tsujii, K. Iitani, P.J. Chien, M. Ye, et al., Real-time monitoring of skin ethanol gas by a high-sensitivity gas phase biosensor (bio-sniffer) for the non-invasive evaluation of volatile blood compounds, Biosens. Bioelectron. 129 (2019) 245–253, https://doi.org/10.1016/j.bios.2018.09.070.

[24] P.J. Chien, T. Suzuki, M. Tsujii, M. Ye, K. Toma, T. Arakawa, et al., Bio-sniffer (gas-phase biosensor) with secondary alcohol dehydrogenase (S-ADH) for determination of isopropanol in exhaled air as a potential volatile biomarker, Biosens. Bioelectron. 91 (2017) 341–346, https://doi.org/10.1016/j.bios.2016.12.050.

[25] M. Ye, P.J. Chien, K. Toma, T. Arakawa, K. Mitsubayashi, An acetone bio-sniffer (gas phase biosensor) enabling assessment of lipid metabolism from exhaled breath, Biosens. Bioelectron. 73 (2015) 208–213, https://doi.org/10.1016/j.bios.2015.04.023.

[26] T. Kamei, T. Tsuda, Y. Mibu, S. Kitagawa, H. Wada, K. Naitoh, et al., Novel instrumentation for determination of ethanol concentrations in human perspiration by gas chromatography and a good interrelationship between ethanol concentrations in sweat and blood, Anal. Chim. Acta 365 (1998) 259–266, https://doi.org/10.1016/S0003-2670(97)00673-9.

[27] H. Kudo, M. Sawai, Y. Suzuki, X. Wang, T. Gessei, D. Takahashi, et al., Fiber-optic bio-sniffer (biochemical gas sensor) for high-selective monitoring of ethanol vapor using 335 nm UV-LED, Sensor. Actuator. B Chem. 147 (2010) 676–680, https://doi.org/10.1016/j.snb.2010.03.066.

[28] G. Konvalina, H. Haick, Sensors for breath testing: from nanomaterials to comprehensive disease detection, Acc. Chem. Res. 47 (2014) 66–76, https://doi.org/10.1021/ar400070m.

[29] K. Naitoh, Y. Inai, T. Hirabayashi, T. Tsuda, Direct temperature-controlled trapping system and its use for the gas chromatographic determination of organic vapor released from human skin, Anal. Chem. 72 (2000) 2797–2801, https://doi.org/10.1021/ac9913309.